3rd URSI AT-AP-RASC, Gran Canaria, 29 May – 3 June 2022

Fully Passive Multi-rectenna Channel Estimation for Microwave Wireless Power Transfer

Kentaro Murata*, Shinnosuke Kondo and Naoki Honma
Iwate University, Morioka, Iwate 020-8551 Japan

Abstract

An inevitable dilemma exists concerning microwave wireless power transfer. If a receiver fails to send a pilot signal, the transmitter array cannot perform channel estimation, resulting in unsuccessful efficient energy beamforming. This study proposes a novel channel estimation method for multiple rectennas with an ultimately simple configuration, i.e., a rectifier only, wherein a pseudo-load modulation based on rectenna non-linearity and full utilisation of power-spatial degrees of freedom is performed, thus making it possible to extract and separate the inherently coherent backscattered waves. A statistical evaluation of the experiments using a 16-element array and dual fully passive rectennas was conducted in a shielded room. The proposed method was found to successfully achieve a channel estimation accuracy of 97.5%, comparable with ideal backscattering modulation.

1 Introduction

Expectations for the realisation of microwave wireless power transfer (MWPT) technology to cut the "last wire" for power supply and management of IoT devices is increasing. For high-efficiency MWPT, beamforming (BF) is performed based on the channel information estimated via pilot signalling from rectennas [1, 2]. Conversely, if the rectenna has a dead battery or no communication functionality, high-efficiency BF becomes extremely difficult; this is one of the major barriers to realising MWPT.

To solve this dilemma, rectenna finding methods have been proposed, as summarised in Table 1. First, *backscattering (BS)* [3,4] performs rectenna channel estimation through the load modulation of an externally emitted pilot signal, thus eliminating an active signal source on the rectenna. However, it still requires extra power to drive the modulator and controller. Second, *received signal strength (RSS)-based frequency modulation* [5] can selectively wake up battery-less multiple rectennas using an activation circuit triggered by multi-tone intermodulation and track them by monitoring the backscattered modulation frequency of a 3.6-GHz band produced by a voltage-controlled oscillator, whereas beam-scanning in a 5.8-GHz band can perform power-adaptive BF depending on rectenna locations. Despite the sophisticated MWPT design, it requires many devices in addition to the rectifier, increasing the rectenna hardware complexity. Third, *harmonic feedback* [6, 7] utilising harmonic re-radiation from the rectenna allows rectenna finding using simple configurations with only passive antenna and microwave components. However, harmonics re-radiation leads to the degradation of power conversion efficiency (PCE). Moreover, the use of the frequency degree of freedom (DoF) potentially interferes with other wireless systems and suffers from frequency-dependent multi-path fading.

Table 1. Comparison of state-of-the-art rectenna finding methods for MWPT of constraints on rectennas.

Method [reference]	Extra power	Extra hardware	Extra frequency	Multi-path	Multi-rectenna
Backscatter [3, 4]	**Need**	**Modulator Controller**	Narrowband	No affect	Support
RSS-based freq. mod. [5]	No need	**Ext. ant. Modulator Oscillator Activ. circ.**	**Dual band Multi-tone Freq. mod.**	**Affect**	Support
Harmonic feedback [6, 7]	No need	Ext. ant. Duplex ant. Coupler	**Harmonics**	**Affect**	**No support**
This work	**No need**	**Rectifier only**	**Fund. CW only**	**No affect**	**Support**

To overcome the above trade-off, this study proposes a fully passive channel estimation method that is scalable to multiple rectennas using only a fundamental continuous wave (CW): First, the incident power-dependent pseudo-load modulation based on rectenna non-linearity extracts a coherent backscattered wave [8]. Second, the full utilisation of the power-spatial DoF separates the backscattered wave into desired multiple signals from the rectennas. This study also explains the theory of the proposed method and reports the experimental demonstration of its superiority.

2 Proposed method

Fig. 1 conceptually illustrates the proposed method. In the system, in addition to the N-element active-phased array for MWPT, a CW pilot signal transmitter (Tx) is assumed. The array can switch transmission/reception modes, and when the Tx transmits a pilot signal, it operates as a receiver (Rx) for channel estimation by receiving backscattered signals from multiple rectennas, that is, the scatterers (Sxs). After channel estimation, it switches to the transmission mode and performs BF based on the estimated channel information. Although the following explanation assumes dual rectennas for simplicity, the proposed method can be applied to more

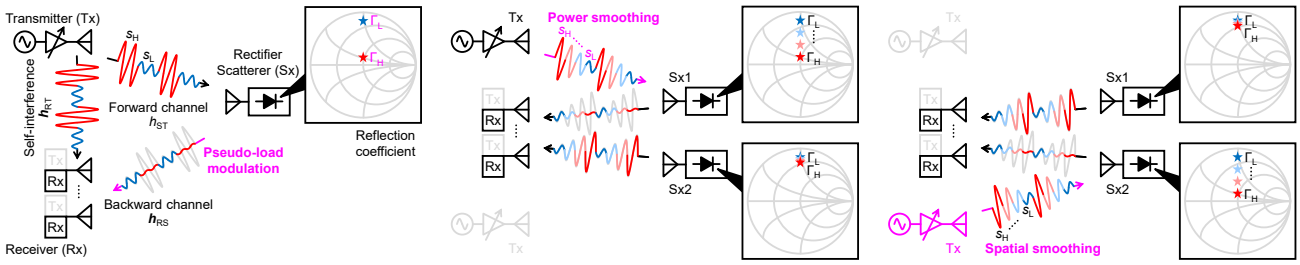

(a) Pseudo-load modulation. (b) Power smoothing. (c) Spatial smoothing.

Figure 1. Conceptual sketch of proposed fully passive multi-rectenna channel estimation method.

than two in principle. In the following, $|\cdot|$, $(\cdot)^*$, $(\cdot)^H$, $\|\cdot\|_F$, and $E[\cdot]$ denote the absolute, complex conjugate, Hermitian transpose, Frobenius norm, and time average, respectively.

The proposed method is based on the conventional method shown in Fig. 1(a), utilising the non-linearity of the rectenna reflection coefficient to the incident power to extract the rectenna backscattered waves [8]. More specifically, let the reflection coefficients of Sxm (m =1, 2) for the high/low pilot signals s_{H} and s_{L} be $\Gamma_{\mathrm{H},m}$ and $\Gamma_{\mathrm{L},m}$, respectively, and the binary received signal vectors are given as

$$\begin{aligned} \boldsymbol{y}_{\mathrm{H}} &= \left(\boldsymbol{h}_{\mathrm{RT}} + \boldsymbol{h}_{\mathrm{RS},1}\Gamma_{\mathrm{H},1}h_{\mathrm{ST},1} + \boldsymbol{h}_{\mathrm{RS},2}\Gamma_{\mathrm{H},2}h_{\mathrm{ST},2}\right) s_{\mathrm{H}} \\ \boldsymbol{y}_{\mathrm{L}} &= \left(\boldsymbol{h}_{\mathrm{RT}} + \boldsymbol{h}_{\mathrm{RS},1}\Gamma_{\mathrm{L},1}h_{\mathrm{ST},1} + \boldsymbol{h}_{\mathrm{RS},2}\Gamma_{\mathrm{L},2}h_{\mathrm{ST},2}\right) s_{\mathrm{L}} \end{aligned} \tag{1}$$

where a mutual coupling between Sxs and noise at Rx are assumed negligible for simplicity.

In the brackets of (1), the first term $\boldsymbol{h}_{\mathrm{RT}} \in \mathbb{C}^N$ represents the self-interference channel between Tx/Rx, including direct and environmentally scattered waves, which does not vary with changes in the pilot signal level. In contrast, the second and third terms represent backscattered channels of the rectennas via the forward channel $h_{\mathrm{ST},m} \in \mathbb{C}$ between Tx/Sxm and backward channel $\boldsymbol{h}_{\mathrm{RS},m} \in \mathbb{C}^N$ between Sxm/Rx, which vary non-linearly with pilot signal levels and behave as if they were pseudo-load-modulated. Thus, considering the ratio of the high/low pilot signals, self-interference cancellation (SIC) can be performed by digital subtraction of the received signals in (1) as

$$\Delta\boldsymbol{y} = \boldsymbol{y}_{\mathrm{H}} - \boldsymbol{y}_{\mathrm{L}}\frac{s_{\mathrm{H}}}{s_{\mathrm{L}}} = \left(\Delta\Gamma_1 h_{\mathrm{ST},1}\boldsymbol{h}_{\mathrm{RS},1} + \Delta\Gamma_2 h_{\mathrm{ST},2}\boldsymbol{h}_{\mathrm{RS},2}\right) s_{\mathrm{H}} \tag{2}$$

where $\Delta\Gamma_m = \Gamma_{\mathrm{H},m} - \Gamma_{\mathrm{L},m}$ is the reflection coefficient difference, and only backscattered channels were extracted.

However, two backscattered signals from Sx1, 2 in (2) are still regarded as instantaneously combined coherent signals. For example, the correlation matrix of the subtracted received signal is analysed as:

$$\boldsymbol{R} = E\left[\Delta\boldsymbol{y}\Delta\boldsymbol{y}^H\right] = \boldsymbol{R}_{11} + \boldsymbol{R}_{22} + \boldsymbol{R}_{12} + \boldsymbol{R}_{21} \tag{3}$$

where

$$\begin{aligned} \boldsymbol{R}_{11} &= E\left[|\Delta\Gamma_1 h_{\mathrm{ST},1}s_{\mathrm{H}}|^2\right]\boldsymbol{h}_{\mathrm{RS},1}\boldsymbol{h}_{\mathrm{RS},1}^H \\ \boldsymbol{R}_{22} &= E\left[|\Delta\Gamma_2 h_{\mathrm{ST},2}s_{\mathrm{H}}|^2\right]\boldsymbol{h}_{\mathrm{RS},2}\boldsymbol{h}_{\mathrm{RS},2}^H \\ \boldsymbol{R}_{12} &= \boldsymbol{R}_{21}^H = E\left[\Delta\Gamma_1\Delta\Gamma_2^* h_{\mathrm{ST},1}h_{\mathrm{ST},2}^*|s_{\mathrm{H}}|^2\right]\boldsymbol{h}_{\mathrm{RS},1}\boldsymbol{h}_{\mathrm{RS},2}^H. \end{aligned}$$

In (3), the cross-correlation matrices $\boldsymbol{R}_{12}$ and $\boldsymbol{R}_{21}$ must be a zero matrix for the backscattered signals to be uncorrelated. However, the backscattered signals from Sx1, 2 are perfectly correlated, sharing the pilot signal s_{H} from the common source. Therefore, the proposed method decorrelates the backscattered waves by utilising the power and spatial DoFs.

First, focusing on the cross-correlation of the reflection coefficient differences $\Delta\Gamma_1\Delta\Gamma_2^*$ in (3), a pilot signal sweeping with multi-level yields a variety of changes in the rectenna reflection coefficients, as shown in Fig. 1(b). Averaging the correlation matrices in the power axis can reduce the cross-correlation factor $\Delta\Gamma_1\Delta\Gamma_2^*$; this process is called power smoothing. Second, focusing on the cross-correlation of the forward channels $h_{\mathrm{ST},1}h_{\mathrm{ST},2}^*$ in (3), a pilot signalling from multi-Tx yields a variety of changes in the forward channels, as shown in Fig. 1(c). This also gives an additional change in the incident power to the rectennas, which has a synergistic effect of further changing the reflection coefficient and compensating for the positional gap. Thus, averaging the correlation matrices in the spatial axis can reduce cross-correlation factors, not only $h_{\mathrm{ST},1}h_{\mathrm{ST},2}^*$ but also $\Delta\Gamma_1\Delta\Gamma_2^*$. This is inspired by well-known spatial smoothing.

To summarise, suppose an arbitrary high/low pilot signal pair is chosen among P pilot signals from Q Txs, a total of ${}_P C_2 Q$ combinations of subtracted received signals exists. Let the subtracted received signal for the pth pair of high/low pilot signals from the qth Tx be $\Delta\boldsymbol{y}_{pq}$, and the correlation matrix with the power-spatial smoothing (PSS) is given as

$$\boldsymbol{R}_{\mathrm{PSS}} = \frac{1}{{}_P C_2 Q}\sum_{p=1}^{{}_P C_2}\sum_{q=1}^{Q}\Delta\boldsymbol{y}_{pq}\Delta\boldsymbol{y}_{pq}^H. \tag{4}$$

Finally, the eigenvalue decomposition of (4) provides a set of primary and secondary eigenvectors $\hat{\boldsymbol{V}} \in \mathbb{C}^{N\times 2}$ spanning the signal space of the channel matrix $\boldsymbol{H}_{\mathrm{RS}}$ of Sx1, 2, which can be used for BF as the estimated channel information.

3 Experimental result

A schematic of the experimental system is presented in Fig. 2(a). The experiment was conducted in a shielded room 3 m wide, 5 m deep, and 3 m high. Identical patch antennas with the gain of about 9 dBi were used for the Tx1-4, Sx1, 2, and a half-wavelength-spaced 16-element patch array of the typical element gain of 5.64 dBi was used for the Rx.

For the Tx side, the vector network analyser (VNA) port P1 was used as a CW pilot signal source with a frequency 2.4 GHz. The signal power was boosted using the amplifier, input to either of the Tx1-4 via the SP4T switch and swept from 30 to 0 dBm in 1-dB steps using the variable attenuator to implement the proposed method. A small portion of the signal was input to P2 via the directional coupler to measure the pilot signal online for the SIC. For the Rx side, P3 acquires the received signal vector by high-speed switching the Rx array elements #1-16 with the SP16T switch. For the Sx side, the loads of Sx1 and 2 were changed via the SPDT switches: first, P4, 5 were connected to measure the true channel matrix $\boldsymbol{H}_{\mathrm{RS}}$ between Rx/Sx1, 2 for evaluation purposes. Second, one was switched to the normally open end and the other to the matched VNA port, alternatively, to perform ideal on-off keying (OOK) BS modulation for comparison. Third, the respective rectifiers were connected to investigate the performance of the proposed method.

A Cartesian coordinate was defined with the origin just below the Rx array, and the Tx1-4 were symmetrically placed around the Rx, as shown in Fig. 2(b). Sx1, 2 were positioned at either of the five spots (green) and 15 spots (yellow), respectively, as shown in Fig. 2(c) and connected to half-wave (HW) or full-wave (FW) rectifier: Thus, a total of 300 measurements were carried out with different Sxs' setting.

As experimental samples for the proposed channel estimation, two HW and two FW rectifiers [9] were fabricated, as shown in Figs. 2(d) and (e), respectively. The Smith charts show that the reflection coefficients of all rectifiers varied non-linearly with the input power change. For reference, the maximum PCEs of the HW and FW rectifiers were 53.9% at 5-dBm input and 53.6% at 13-dBm input, respectively.

Fig. 3 shows channel estimation accuracy versus Sx2's position, when the Sx1 was fixed at $(X, Y) = (-0.5, 2.0)$ m, and FW and HW rectifiers were connected to Sx1, 2, respectively. The channel estimation accuracy is defined as

$$\rho^2 = \frac{\|\hat{\boldsymbol{V}}^H \boldsymbol{H}_{\mathrm{RS}}\|_F^2}{\|\boldsymbol{V}^H \boldsymbol{H}_{\mathrm{RS}}\|_F^2}. \tag{5}$$

In (5), the denominator represents the sum of the RF received power at Sx1, 2 when BF is performed using each eigenvector of $\boldsymbol{V}$ spanning the signal space of the true channel matrix $\boldsymbol{H}_{\mathrm{RS}}$, whereas the numerator indicates that BF is performed using each estimated eigenvector of $\hat{\boldsymbol{V}}$. That is, the closer ρ is to unity, the less unwanted power input to the noise space and the more power input to the signal space. The following compares the five different approaches:

RAND [4] randomly generated independent and identically distributed channel matrices, and the average channel estimation accuracy was evaluated. The very low accuracy shown in Fig. 3(a) implies that high transfer efficiency cannot be achieved by random BF. *Near-field focusing (NFF)* [10] used the set of spherical-wave mode vectors considering path loss calculated from the relative antenna position

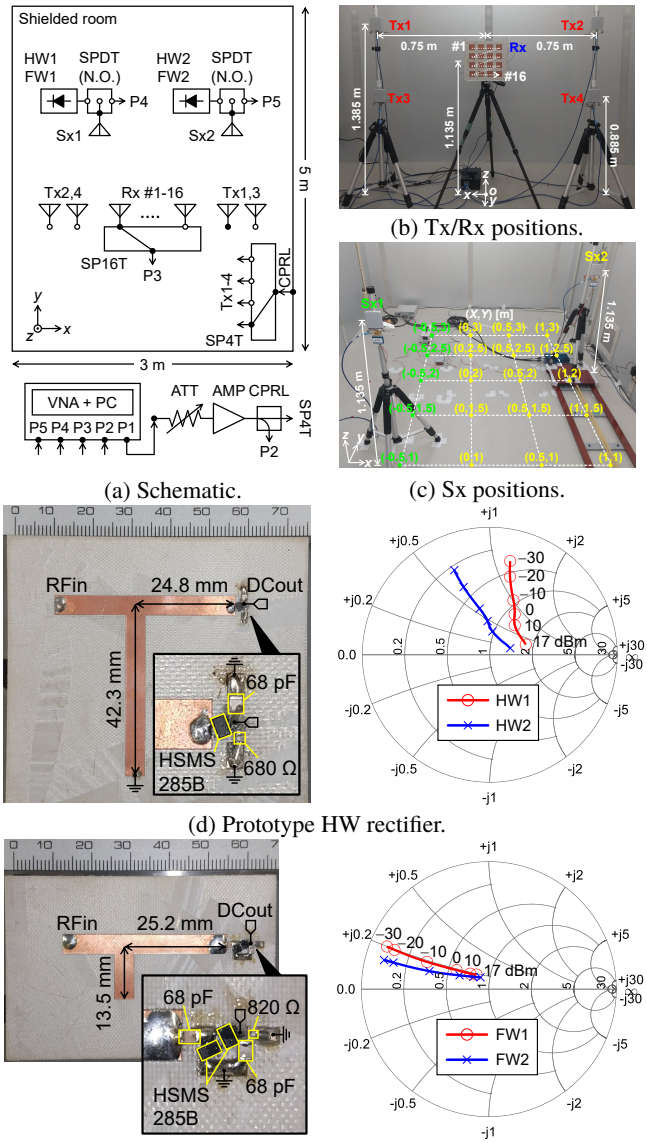

(a) Schematic.

(b) Tx/Rx positions.

(c) Sx positions.

(d) Prototype HW rectifier.

(e) Prototype FW rectifier.

Figure 2. Experimental setup.

as the channel matrix. Despite the accurate positioning and rigorous array calibration, Fig. 3(b) confirms the accuracy degradation owing to the multi-path waves except for near-field and line-of-sight cases, which indicate that the use of frequency DoF [5–7] could also be affected by the multi-path fading. *BS* [3] estimated the channel matrix based on the ideal OOK BS modulation. Although Fig. 3(c) confirms almost perfect estimation at all points, this requires special hardware and active processing for modulation.

In contrast, both *conventional* [8] and *proposed* used a fully passive rectenna configuration and calculated the estimation accuracies from the correlation matrices before and after PSS in (3) and (4), respectively. A comparison with Figs. 3(d) and (e) shows the proposed method offered higher accuracy than the conventional at all points, which proved that the PSS succeeded in the decorrelation of the inherently perfect-correlated rectenna backscattered waves.

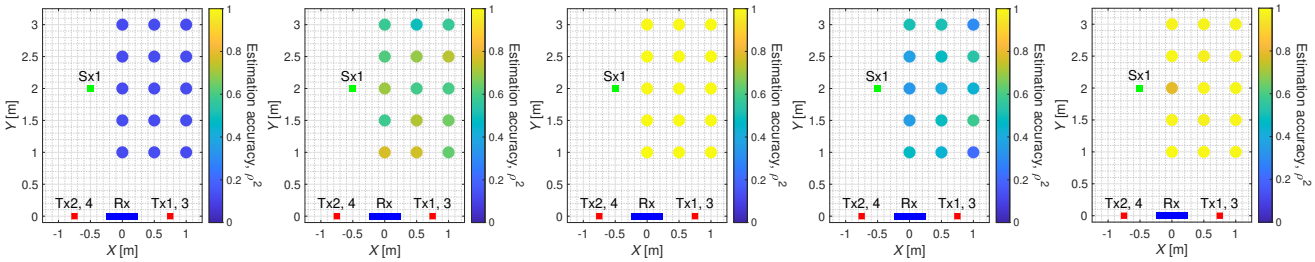

(a) RAND [4]. (b) NFF [10]. (c) BS [3]. (d) Conventional [8]. (e) Proposed.

Figure 3. Estimation accuracy for different Sx2 positions; The rectangular markers represent the positions of Tx1-4, Rx and Sx1, and the circle marker and its hue represent the Sx2 position and the value of estimation accuracy.

Fig. 4 shows the cumulative distribution functions (CDFs) of the estimation accuracies for all 300 measurements with different rectenna settings. This statistics shows that the proposed method improved the median by 50.4%pt compared with the conventional and achieved a high accuracy of 97.5% equivalent to BS even with fully passive rectennas.

4 Conclusion

This study proposes a fully passive multi-rectenna channel estimation method for MWPT. The pseudo-load modulation utilising the rectenna non-linearity and PSS realises the extraction and separation of the inherently coherent rectenna backscattered waves from a mixed signal buried in self-interference. The experiment in the multi-path environment demonstrated successful channel estimation of dual rectennas using the proposed method with high accuracy comparable with the ideal BS even with fully passive rectennas.

5 Acknowledgements

This work was supported by JSPS KAKENHI Grant Numbers JP19K23506, JP20K14730, and Strategic Professional Development Program for Young Researchers from MEXT.

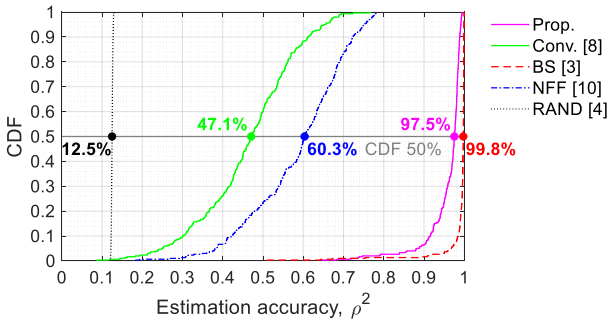

Figure 4. CDF of estimation accuracy for all measurements.

References

[1] K. Murata, T. Mitomo, M. Higaki, and K. Onizuka, "A 5.8-GHz 64-channel phased array microwave power transmission system based on space-time beamforming algorithm for multiple IoT sensors," *EuMC*, 2018.

[2] G. Pabbisetty, K. Murata, K. Taniguchi, T. Mitomo, and H. Mori, "Evaluation of space time beamforming algorithm to realize maintenance-free IoT sensors with wireless power transfer system in 5.7-GHz band," *IEEE Trans. Microw. Theory Techn.*, vol. 67, no. 12, pp. 5228–5234, 2019.

[3] D. Arnitz and M. S. Reynolds, "Multitransmitter wireless power transfer optimization for backscatter RFID transponders," *IEEE Antennas Wireless Propag. Lett.*, vol. 12, pp. 849–852, 2013.

[4] ——, "Wireless power transfer optimization for nonlinear passive backscatter devices," *IEEE RFID*, 2013.

[5] D. Belo, D. C. Ribeiro, P. Pinho, and N. Borges Carvalho, "A selective, tracking, and power adaptive far-field wireless power transfer system," *IEEE Trans. Microw. Theory Techn.*, vol. 67, no. 9, pp. 3856–3866, Sep. 2019.

[6] S. D. Joseph, Y. Huang, S. S. H. Hsu, A. Alieldin, and C. Song, "Second harmonic exploitation for high-efficiency wireless power transfer using duplexing rectenna," *IEEE Trans. Microw. Theory Techn.*, vol. 69, no. 1, pp. 482–494, Jan. 2021.

[7] H. Zhang, Y.-X. Guo, S.-P. Gao, Z. Zhong, and W. Wu, "Exploiting third harmonic of differential charge pump for wireless power transfer antenna alignment," *IEEE Microw. Wireless Compon. Lett.*, vol. 29, no. 1, pp. 71–73, Jan. 2019.

[8] S. Kondo, S. Odajima, K. Murata, and N. Honma, "Passive channel estimation technique for microwave wireless power transfer," *ISAP*, 2021.

[9] C. R. Valenta and G. D. Durgin, "Harvesting wireless power: Survey of energy-harvester conversion efficiency in far-field, wireless power transfer systems," *IEEE Microw. Mag.*, vol. 15, no. 4, pp. 108–120, Jun. 2014.

[10] X. Yi, X. Chen, L. Zhou, S. Hao, B. Zhang, and X. Duan, "A microwave power transmission experiment based on the near-field focused transmitter," *IEEE Antennas Wireless Propag. Lett.*, vol. 18, no. 6, pp. 1105–1108, 2019.